Second International Conference on Microstructural-related Durability of
Cementitious Composites, 11-13 April 2012, Amsterdam, The Netherlands

MULTICOMPONENT MODELLING OF PORTLAND CEMENT HYDRATION REACTIONS

N. Ukrainczyk (1), E.A.B. Koenders (1,2), K. van Breugel (1)

(1) Dep. of Materials & Environment, Delft University of Technology, The Netherlands
(2) COPPE-UFRJ, Universidade Federal do Rio de Janeiro, Brasil

Abstract

The prospect of cement and concrete technologies depends on more in depth understanding of cement hydration reactions. Hydration reaction models simulate the development of the microstructures that can finally be used to estimate the cement based material properties that influence performance and service life. In this paper the multicomponent model of portland cement hydration reactions is implemented within the original Hymostruc model. The reaction kinetics of the four principal clinker minerals, C_3S, C_2S, C_3A, C_4AF, are coupled to the microstructure development. The nature of ettringite transformation to monosulfate is described by sequential chemical reactions of aluminate bearing clinker minerals. The calculated results of the model are shown and compared with systematic literature experimental results investigating the hydration of two different ordinary portland cements. Good agreement was obtained for the component fractional evolution and released heat during hydration.

1. INTRODUCTION

Concrete, the most extensively used man-made construction material, needs to be made more durable and sustainable in order to satisfy socio-economic needs with the least impact to the environment. More and more it is realized that the future of the cement and concrete technologies depends on in depth understanding of cement hydration reactions that result in a development of the microstructure. Cement hydration is a simple technological phenomenon driven by a very intricate chemical reaction process. It comprises of many chemical reactions involving dissolution and precipitation that are moreover intermeshed with interactions and synergies amongst these individual reactions. To deal with this complexity, the modeling of hydration reactions calls for a wise simplification of the real hydration process. A widely employed first approximation approach is to model the hydration of principal anhydrous minerals separately, supposing that the overall hydration reaction is equivalent to the sum of individual reactions. However, it is known that the reaction kinetics of individual anhydrous minerals depends on the composition of the initial mixture (e.g. C_3A hydration accelerates the hydration of C_3S [1,2]). An adequate hydration simulation software backed up with experimental observations presents a tool that can be used to grasp the nature of such intricate interactions. Therefore, it is necessary to have a robust cement hydration reaction model that

can simulate the evolution of the reactants and hydration products during hydration. This can be achieved by describing the most important parts of the hydration phenomenon and relaying on a set of systematic experimental data such as component content evolution (anhydrous cement minerals, free water, and forming hydration products), released heat, chemical shrinkage, strength, etc. Firstly, this model can be tested on a few specific cases (e.g. case studies for given mixture compositions and conditions of hydration). Thereof, one can proceed with generalization to capture the principal correlations and interactions among parameters and variables. In that way the interpolative predictions (simulations) can be made that are valid for a wide range of mixture compositions and hydration conditions. Thankfully, experimental data that include the monitoring of simultaneous phenomenon that occur due to hydration reactions are made more and more available in recent literature. *In situ,* non-destructive high resolution experimental methods are of special interest here, such as quantitative X-ray diffraction (QXRD) and (environmental) scanning electron microscope (SEM). Main motivation behind the development of this multicomponent hydration model is to simulate the development of the microstructures that can finally be used to estimate the material properties that influence performance and service life. Microstructure evolution of the cement based material is obtained through knowledge of hydration reactions (thermodynamics and kinetics). Furthermore, kinetics of the hydration reactions depends again on the microstructure development. This paper describes the multicomponent (C_3S, C_2S, C_3A, C_4AF) model of the portland cement hydration reactions implemented within the original Hymostruc model where the hydration kinetics is internally coupled with the microstructure development.

2. MODELING APPROACH

In Hymostruc the hydration of the individual particles are modeled explicitly in two ways regarding the filling of the system with particles: 1) an original statistically-based cell concept [3] and a full 3D random based approach [4]. The multicomponent chemical model presented in this paper is implemented in both kernels. There are minor difference in numerical results between them; here only statistical approach results are presented. Hydration kinetics is coupled to the microstructure evolution via the basic reaction rate equation (Fig 1). Virtual microstructure of cement paste is recognized as a system of four main (unhydrated) clinker components, hydration products and pores (whether saturated or not with liquid water). The virtual microstructure development during cement hydration is iteratively followed up in order to obtain the basic kinetic equation parameters. The modeling was done with the following assumptions. Each cement grain contains four main clinker minerals (Fig 1b) that react by following hydration reactions. Reactions of silicate clinker minerals are summarized as:

$$C_bS+(b-(C/S)+x)H \rightarrow C_{C/S}SH_x+(b-(C/S))CH \quad (1)$$

where b = 2 or 3 represents reaction of C_3S or C_2S, respectively. For the numerical calculations in this paper C/S = 1.8 and x = 4 is adopted. Reactions of aluminate-bearing clinker minerals are represented by the following sequential chemical reaction schemes:

$$C_3A+3CsH_2+26H \rightarrow C_6As_3H_{32} \quad (2)$$

$$C_3A+0.5C_6As_3H_{32}+2H \rightarrow 1.5\,C_4AsH_{12} \quad (3)$$

$$C_3A+6H \rightarrow C_3AH_6 \quad (4)$$

$$C_4AF+3CsH_2+30H \rightarrow C_6As_3H_{32}+CH+FH_3 \quad (5)$$

$$C_4AF+0.5C_6As_3H_{32}+6H \rightarrow 1.5C_4AsH_{12}+CH+FH_3 \quad (6)$$

$$C_4AF+10H \rightarrow C_3AH_6+CH+FH_3 \quad (7)$$

When all gypsum is consumed ettringite transforms to monosulfate according to eqs. (3 and 6). After both gypsum and ettringite are consumed, the remaining aluminates react according to eqs. (4 and 7).

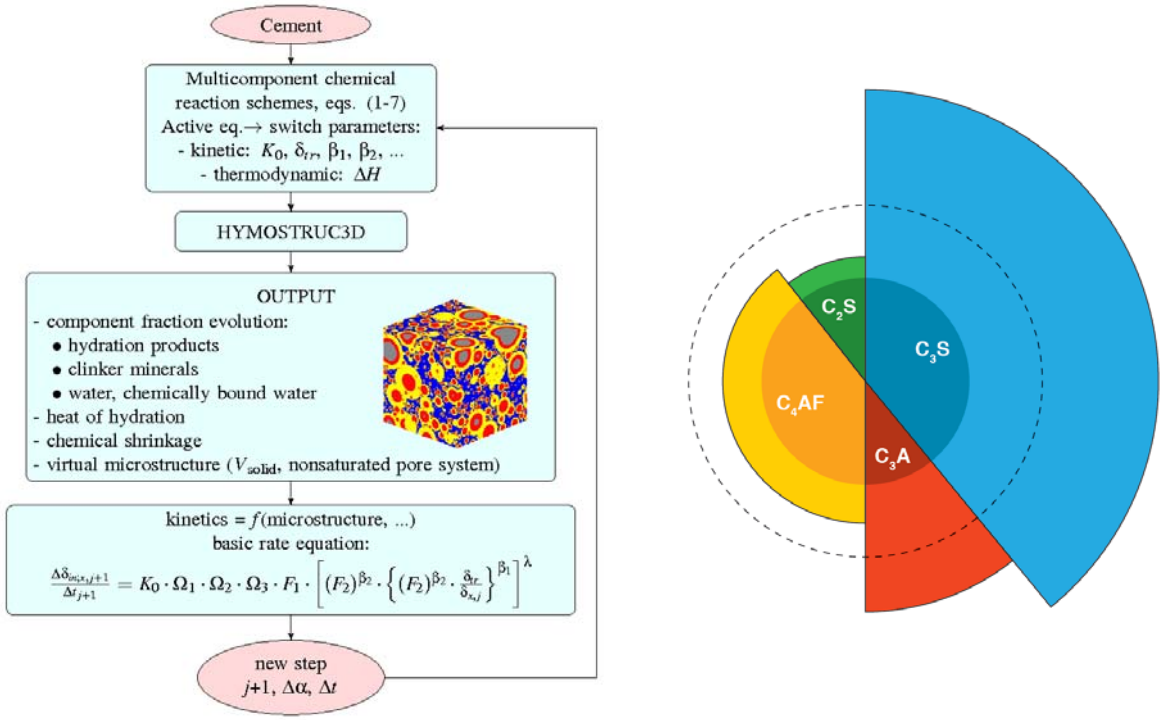

a) b)

Fig 1. Multicomponent reaction concept: a) flow chart; b) independent reactions and an averaged particle growth (dashed line).

The degree of hydration is calculated for each clinker mineral in each time step, and then avaraged by weight to obtain overall hydration degree of the paste. In the same way a particle expansion is calculated from contributions of each clinker minerals (Fig 1a and b). The outer expansion of the particles is calculated according to the so-called particle expansion mechanism [3]. The expansion mechanism describes the outer growth of a spherical central particle, while considering the averaged contribution of all the clinker minerals. The outer growth of the particle expansion can be calculated from a mass balance concept. In this paper we consider only silicate reactions (eq. (1)). The aluminate-bearing clinker minerals, i.e. C_3A and C_4AF, are not considered in this mass-balance-based outer growth concept. The next step in this research is to include the volume expansion of particles due to hydration reactions of non-silicate clinker minerals. The microstructure development is the central part of the model, from which the microstructural properties and reaction kinetics are calculated. The rate of penetration of the reaction front in an individual cement particle x at time t_j is calculated with a Hymostruc basic rate equation (Fig 1), where K_0 is the basic rate factor (μm/h), δ_{tr} the transition thickness (μm) of a hydration product layer ($\delta_{x,j}$) at which the reaction for the individual particle changes from a phase boundary (λ = 0) to a diffusion controlled mechanism (λ = 1). The rate of the reaction process is driven by the initial rate of penetration

which is reduced by three so-called reduction coefficients, Ω_1, Ω_2 and Ω_3, representing the reduction of water withdrawal of particles in the shell of a central cement particle, the reduction of the available water while emptying of the capillary pores, and the water shortage of the overall system, respectively. A detailed description of the original Hymostruc model is given in [3]. The transition thickness kinetic parameters, δ_{tr} can be considered in two simulation scenarios. The first mimics the independent influence of δ_{tr} on each chemical reaction kinetics, while the second takes an overall weighted avarage influence on individual kinetics (Fig 1). The first approach enables to describe the independent kinetics by selective formation of hydration products on top of the corresponding anhydrous clinker minerals. The second approach assumes that the hydration products are distributed heterogeneously on all anhydrous clinker minerals as a shell with an averaged thickness. For modelling, each hydration reaction (1-7) was considered to have a corresponding set of kinetic (K_0, δ_{tr}, β_1 and β_2) and thermodynamic (heat of hydration, ΔH) input parameters. The corresponding parameters switch depending on which of the sequential reaction eq. (2, 3 or 4, and 5, 6 or 7) is active at certain time step. The switch is done when the gypsum or ettringite is completely consumed.

2.1 Validation of the model

Modeling results are validated against the experimental measurements taken from the work of Bullard *et al.* [5]. They reported systematic measurement results made on two different proficiency samples of ordinary portland cement issued by the Cement and Concrete Reference Laboratory (CCRL), designed as CCRL 151 and CCRL 168. Composition of some major components in investigated cements is given in Table 1. The principal differences in the two cements are higher amounts of C_2S and C_3A, MgO and K_2O, and significantly lower amounts of C_3S and C_4AF in CCRL 168. Rosin-Rammler function was used to input the particle size distribution, with the fitted parameters as shown in Fig 2. CCRL 168 is finer than CCRL 151. Particle size range modeled is 1-90 μm. Kinetic input parameter values for the hydration simulation are shown in Table 2. The results are presented in Figs 2-4.

Table 1: Composition of major components in investigated cements (mass %).

Minerals	C_3S	C_2S	C_3A	C_4AF	CsH_2	$CsH_{0.5}$	Cs	$(K,Na)SO_4$
CCRL 151	70.4	9.2	4.4	11.4	1.0	2.9	0.36	0.72
CCRL 168	54.5	15.7	8.0	7.0	-	2.25	0.19	2.85

Chemical composition	CaO	SiO_2	Al_2O_3	Fe_2O_3	MgO	K_2O	Na_2O	Total SO_3	SO_3 in clinker solid solution
CCRL 151	64.73	20.03	4.91	3.46	1.34	0.32	0.27	3.12	0.45
CCRL 168	62.28	19.91	5.11	2.14	3.48	1.23	0.23	3.48	0.77

Table 2. Kinetic input values for the hydration simulation (values in parentheses represent values estimated from correlations with corresponding clinker mineral weight fraction [6]).

Reaction eqs.	CCRL 151			CCRL 168		
	K_0	δ_{tr}	β_1 and β_2	K_0	δ_{tr}	β_1 and β_2
(1, b=3) C_3S	0.11 (0.070)	5 (1.8)	2	0.14 (0.073)	6 (1.5)	2
(1, b=2) C_2S	0.025 (0.005)	5 (1.0)	2	0.04 (0.005)	6 (1.2)	2
(2-4) C_3A	0.10 (0.08)	5 (1.1)	2	0.12 (0.14)	6 (1.16)	2
(5-7) C_4AF	0.015	5	2	0.015	6	2

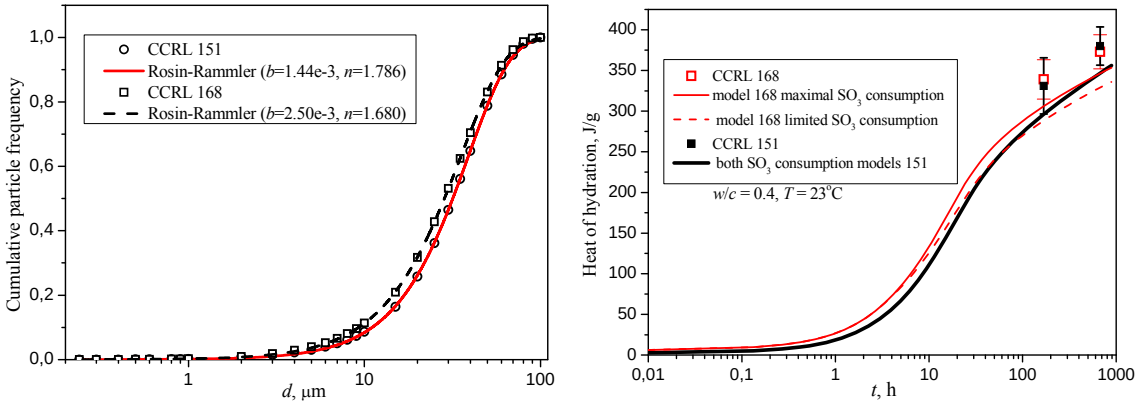

a) b)

Fig 2. Comparison of modeled and expeimental [5] a) particle size distribution b) heat release.

3. RESULTS AND DISCUSSION

The only adjusted parameters for the validation are kinetic parameters K_0 and δ_{tr} for each of the reactions (1-7). As discussed in introduction, kinetic parameters depend on the composition of cement, so are expected to vary for different portland cements. Van Breugel [3] proposed a simple correlation of K_0 and δ_{tr} with a mass fraction of the corresponding clinker mineral (C_3S, C_2S and in [6] also with C_3A), e.g. in a form of $K_0(C_3S) = f(C_3S)$. The interactions are somewhat included indirectly because the higher content of one mineral could reduce others. This correlations could be extended to consider the interactions (synergies) among parameters directly, e.g. $K_0(C_3S) = f(C_3S, C_2S, C_3A, \ldots)$. Values in parentheses in Table 2 represent parameter values calculated from correlations proposed in [6]. There are significant discrepancies between the values adopted in this paper and those predicted by the correlations. This could be attributed to synergy effects that were not included in the correlations. For example, it is known that the C_3A hydration accelerates the hydration of C_3S [1,2]. This feature is clearly captured in this study. Namely, almost doubling of the C_3A content (Table 1) significantly increases the hydration kinetics of C_3S, but also C_2S and C_3A. Furthermore, the discrepancies in kinetic parameters between this study and [6] could also be attributed to experimental conditions that were not taken into account but could influence the hydration reaction kinetics. For instance, an added internal standard (corundum) in prepared cement pastes may change the hydration kinetics (e.g. via heterogeneous nucleation and growth mechanism). Internal standard must be added in QXRD analysis in order to provide a baseline signal for calibrating the XRD signal intensities to volume fractions. The standard can be added directly in paste during mixing, or afterwards during destructive sample preparation for XRD analysis.

3.1 Component weight fraction evolution

During hydration, the microstructure of the material and amounts of certain phases are changing. Volume fractions of reactants, i.e. the non-reacted cement and the free water, decrease, while the total fraction of the formed hydration products increases, during the setting and hardening. The solid fraction comprises the formed hydration products and the fraction of non-reacted cement. Figs 3 and 4 compare the predicted model results against the measured weight fraction evolution of the four principal clinker minerals, gypsum, chemically bound water (denoted as BW) and of major hydration products (CSH gel, CH, ettingite, monosulfate and C_3AH_6).

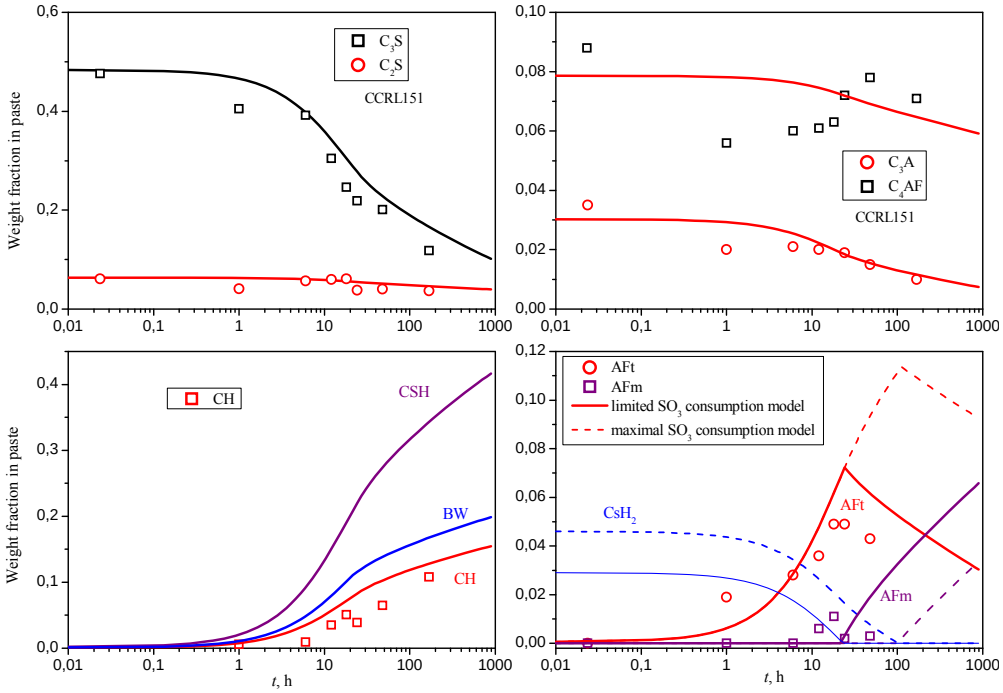

Fig 3. CCRL 151 cement paste weight fraction evolution (w/c=0.45, T=23°C). Comparison of QXRD experimental data [5] with model predictions.

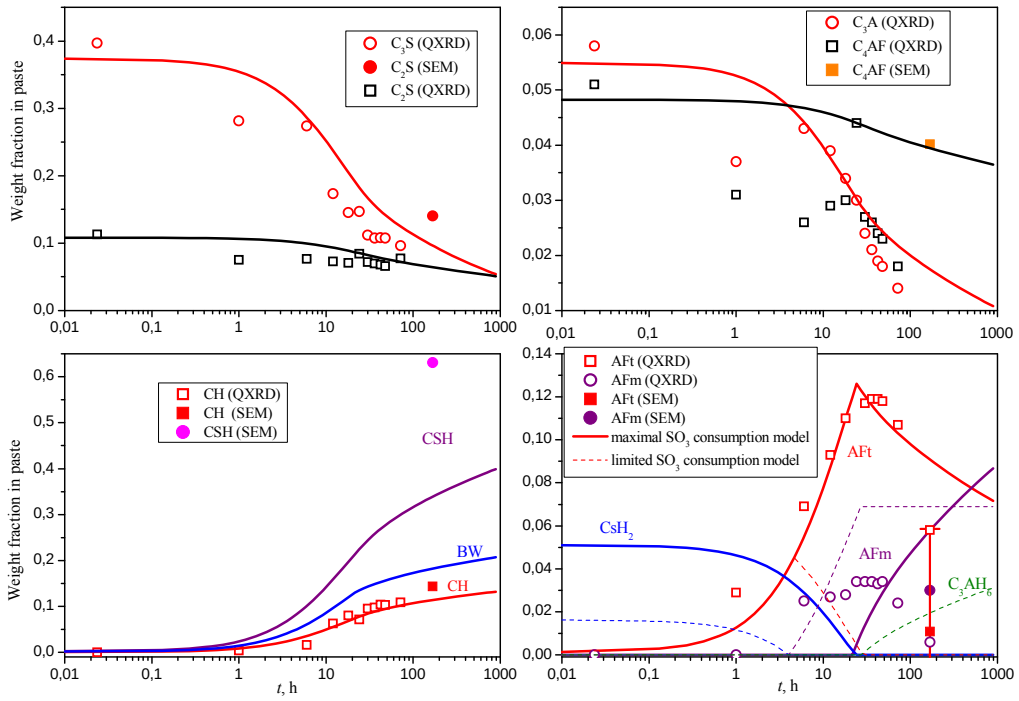

Fig 4. CCRL 168 cement paste weight fraction evolution (w/c=0.45, T=23°C). Comparison of QXRD and QSEM experimental data [5] with model predictions.

The ordinate represents the weight fraction normalized to the total cement paste mass (i.e. cement plus water, without internal standard). The model exhibits a good accord with the experimental data of clinker minerals consumption, except for the C_4AF (which can be attributed to a high scatter of C_4AF experimental data). Furthermore, there is a significant overestimate of the monosulfate after 72 h. The amorphous content of cement paste is considered to be predominantly C-S-H. However, monosulfate (and AFm hydration products

in general) are often weakly crystalline, and therefore may contribute to the total amorphous content estimated that is not visible to XRD. For CCRL 168 there are additional experimental data given by quantitative SEM analysis, shown in Fig 4 as solid (closed) symbols. The model predicts the mass fraction of CH better for CCRL 168 than it does for CCRL 151. At this point the model does not account for the early formation of monosulfate between 8 - 36 h, nor for its apparent disappearance at later ages. In [5,7] the absence of monosulfate in cement pastes was explained by carbonation effect, that finaly tansforms the monosulfate back to ettringite and carbonate AFm hydration products (hemicarbonate or monocarbonate). This carbonation process is not considered in this paper, but can be implemented following the same chemical implementation approach as presented here.

Two models are plotted for the prediction of gypsum, ettringite, monosulfate and hydrogarnet evolution corresponding to calculations with different amounts of SO_3 consumption. The continuous and dashed model lines differentiate in considering: 1) maximal or 2) limited SO_3 consumption, respectively. For the maximal SO_3 consumption model, the amount of available gypsum to form the ettringite is assumed to be 6.708 % and 7.48 % as calculated from the total SO_3 content in cement CCRL 151 and CCRL 168, respectively (given in Table 1). The calculation of available gypsum content from total SO_3 rests on stoichiometry of gypsum (moles of $CaOH_2$ are equal to moles of SO_3):

$$w_{gypsum} = w_{\mathrm{CaO+2H_2O}} + w_{\mathrm{SO_3}} = w_{\mathrm{SO_3}} M_{\mathrm{CaO+2H_2O}} \big/ M_{\mathrm{SO_3}} + w_{\mathrm{SO_3}} = 2.15\, w(\mathrm{SO_3}) \qquad (8)$$

The increased amount of a real gypsum content is justified because the reactions (2 and 5) involve first the dissolution of reactants (gypsum and C_3A) and then precipitation of the hydration product ettringte [8]. So it is in fact the amount of available aqueous species that participate ettringite. Therefore, the amount of 'missing' Ca^{2+} that is not accounted in initial gypsum content could come from free CaO or dissolution of clinker minerals. On the other hand, for the limited SO_3 consumption model, the amount of available gypsum to form the ettringite is assumed to be 4.26 % and 2.44% according to Table 1 (i.e. approximated as a sum of gypsum, hemihydrate and anhydrite), for CCRL 151 and CCRL 168, respectively. Interestingly, the better accord especially regarding to the ettringite evolution in CCRL 151 is obtained considering the maximal SO_3 consumption model, while in CCRL 168 for assuming limited SO_3 consumption. Therefore, one could speculate that in CCRL 151 indeed only gypsum, hemihydrate and anhydrite are involved to form ettringite, while the rest of the SO_3 could be adsorbed on solid particles [8], not yet released from anhydrous particles (because the reaction front (water) did not reach it yet), and/or there is no 'missing' Ca^{2+} so the kinetics is rather slow. On the other side, for CCRL 168 one can explain that excellent fit for maximal SO_3 consumption, and drastic discrepancy for limited SO_3 consumption model, could be due to a formation of ettringite also by consumption of alkali soluble sulphates. Indeed, Table 1 shows much higher amount of alkali soluble SO_3 in CCRL 168 than in CCRL 151.

3.1 Heat of hydration

Experimental data on the heat of hydration at 7 and 28 days for both cements (w/c = 0.4, T = 23°C) taken from [5] are presented in Fig 2b with the error bars representing ± 1 standard deviation. The model predicts the isothermal heat of hydration based on the thermodynamic data for enthalpy change of each reaction [9]. For example, heat release from C_3A reaction at certain time step is calculated from the corresponding theoretical reaction heat multiplied by the hydration degree of the reacting clinker mineral. The corresponding theoretical reaction heat input switches depending on which of the sequential reaction eq. (2, 3 or 4) that is active at certain time step. The switch is done when the gypsum or ettringite is completely

consumed. The overall (multicomponent) heat release is obtained by weight average summation over all clinker minerals. In this paper, heats for C_4AF reactions were not separated into individual eq. (5-7), but were taken to be 725 J/g [9] for all C_4AF reactions. The model predictions are made for a cement paste with w/c=0.4 cured isothermally at T = 23°C. In Fig 2b, the solid and dashed lines correspond to maximal and limited SO_3 consumption model, respectively. For CCRL 151 the calculated heat evolution is almost the same for both (SO_3) models. For CCRL 168 the heat evolution exhibits lower values for the model with lower ettringite content, due the following magnitude of theoretical reaction heats: 1672 J/g (of C_3A) for eq. (2), 880.8 J/g for eq. (3), and 906.7 J/g for eq. (4). The accord with the experimental data is reasonably good, with somewhat underestimate especially for the low ettringite CCRL 168 model.

4. CONCLUSION

Hydration reactions of multicomponent clinker minerals are implemented in the Hymostruc model by coupling reaction kinetics with microstructure development. Sequential chemical reaction scheme was used for aluminate bearing clinker minerals, with internally switching of corresponding parameters. The model predictions show good accord against literature experimental results obtained from QXRD, QSEM and calorimetric investigations of two ordinary portland cement pastes. Prediction of ettringite and monosulfate are highly dependent on amount of available SO_3. Implemented hydration reaction model presents a flexible tool to deal with a complex interactions observed by experiments. Kinetic parameters obtained from literature experimental database should be correlated to a wide range of mixture compositions and hydration conditions. In future work the reactions of aluminate-bearing clinker minerals will be fully taken into account in the microstructural development. The model will be further extended with cements containing supplementary additives (such as fly ash or slag) and towards a microstructural 3D numerical model for effective diffusivity assessment.

ACKNOWLEDGMENTS

This work was supported by the *Marie Curie* Actions EU grant FP7-PEOPLE-2010-IEF-272653-DICEM, the postdoc personal grant from the National Foundation for Science, Higher Education and Technological Development of the Republic of Croatia, and Microlab at Dep. of Materials and Structures, Delft University of Technology.

REFERENCES

[1] Bensted, J., 'Cement Science, Is It Simple? ', *Cement Wapno Beton* **6/67** (1) (2001) 6-19.
[2] Stark, J, Moser, B, Eckart, A, 'New approach to cemen hydration', *ZKG Int.* **54** (2) (2001)114-119.
[3] Breugel, K. Van, Simulation of Hydration and Formation of Structure in Hardening Cement-Based Materials, PhD-Thesis, 1991, TU Delft.
[4] Koenders, E.A.B., Simulation of Volume Changes in Hardening Cement-Based Materials, PhD-Thesis, 1997, TU Delft.
[5] Bullard, J.W., *et* al., 'Coupling thermodynamics and digital image models to simulate hydration and microstructure development of portland cement pastes', *J. Mater. Res.* **26** (4) (2011) 609-622.
[6] Nguyen, V.T., Rice husk ash as a mineral admixture for Ultra High Performance Concrete, PhD-Thesis, 2011, TU Delft.
[7] Brouwers, H.J.H., 'The work of Powers and Brownyard revisited: Part 2', *Cem. Con. Res.* **35** (10) (2005) 1922-1936.
[8] Bullard, J.W. *et* al., 'Mechanisms of cement hydration', *Cem. Con. Res.* **41** (12) (2011) 1208-1223.
[9] Taylor, H.F.W., Cement Chemistry, 1997 Ed. 2, Thomas Telford, London.